https://doi.org/10.48047/AFJBS.6.S13.2024.817-830

African Journal of Biological Sciences

Journal homepage: http://www.afjbs.com

Research Paper Open Access

Inhibition Effect Of $N(CH_3)_4^+OH^-$On the Corrosion Of API 5L X70Steelin 0.5M H_2SO_4: A Detailed Experimental and Computational Methods

LAHOUEL Ali[1,3*], SAOUDI Adel[2], ABDERRAHIM Karima[3], MOUSSAOUI Kamilia[3] and Oday Mohammad Ahmad Khamaysa[4]

[1]Metallurgy and Materials Engineering Department, Badji Mokhtar - Annaba University 12, P.O.BOX, 23000 Annaba, Algeria

[2]Centre de Recherche Scientifique et Technique en Analyses Physico-Chimiques (CRAPC), Zone Industrielle BP 384, Bou-Ismail, Tipaza, Algerie

[3]Surface Engineering Laboratory (L.I.S), Badji Mokhtar –Annaba University.12, P.O.Box, 23000 Annaba, Algeria

[4]Laboratory of Analytical Sciences, Materials and Environmental (LSAME), Larbi BenM'Hidi University, Oum El Bouaghi 04000, Algeria

* Corresponding author.E-mail addresses: karima.abderrahim@univ-annaba.dz(ABDERRAHIM Karima), ali.lahouel@univ-annaba.dz (LAHOUEL Ali)

Article History
Volume 6, Issue 1**3**, 2024
Received: 2 **2**Apr 2024
Accepted: **21** July 2024
doi:
10.48047/AFJBS.6.13.2024.817-830

Abstract

The corrosion inhibition of X70 steel by $N(CH_3)_4^+$ OH^-in 0.5M H_2SO_4 at 298K was investigated through experimental and computational methods. The weight loss method, potentiodynamic polarization, and electrochemical impedance spectroscopy (EIS) were employed to evaluate the inhibition performance of the inhibitor. Theoretical calculations based on molecular dynamics were used to analyze the adsorption behavior of the inhibitor molecules and the interaction between the inhibitor and the steel surface. The results indicated a mixed inhibition mode and an increase in charge transfer resistance due to the adsorption of inhibitor molecules on the steel surface. The calculated inhibition efficiencies show good agreement, with a maximum value of 85.88%. The adsorption follows the Langmuir isotherm. Optical microscopy (OM) observations confirm the presence of an inhibitor film on the steel surface, effectively reducing the corrosion rate. Molecular dynamics simulation reveals that the studied inhibitor molecules were adsorbed nearly to the Fe surface. The adsorption of inhibitors on the Fe (110) surface is spontaneous, strong, and stable.

Keywords: API 5L X70; $N(CH_3)_4^+$ OH^-; Corrosion; Inhibition; EIS; Tafel; Molecular dynamics.

1. Introduction

Steels are widely used as construction materials across various fields, including the medical, automotive, and food industries [1], steam power plants [2], piping systems, chemical plants, and heat exchanger equipment [3]. Their popularity is attributed to their

mechanical strength, durability, and corrosion resistance, primarily due to the formation of a passive oxide film on their surface. However, despite their general corrosion resistance, these steels are vulnerable to corrosion in specific acidic environments [4]. Sulfuric acid and hydrochloric acid, for example, are commonly used for pickling, cleaning, and descaling in industrial processes [5-6], and they pose significant corrosion risks to steel materials.

To mitigate corrosion, the use of organic inhibitors has emerged as a practical, economical, and effective method of protection [7]. Among the various types of inhibitors, heterocyclic organic compounds are particularly noted for their efficacy in protecting mild steel in acidic environments [8]. The adsorption mechanism of these compounds typically involves heteroatoms such as nitrogen, oxygen, and sulfur [9-10]. The effectiveness of these inhibitors depends on several factors, including the physicochemical properties of the inhibitor, the chemical composition of the electrolyte, and the nature of the metal [11-12].

Tetramethylammonium hydroxide (TMAOH) and its derivatives are among the organic compounds identified as effective inhibitors against the corrosion of mild steels in hydrochloric acid [13-20]. These compounds prevent corrosion and play a significant role in biological activities due to their presence in natural and pharmaceutical products. TMAOH and its derivatives generally possess various pharmacological properties [13,21], adding to their utility.

Despite their potential, limited research has been done on using TMAOH and its derivatives as corrosion inhibitors for steels [22]. This gap in the literature highlights the need for further investigation into their effectiveness and mechanisms of action.

In this study, we aim to address this gap by exploring the corrosion inhibition of API 5L X70 steel using $N(CH_3)_4^+$ OH^-in 0.5M H_2SO_4. This work involves comprehensive monitoring of corrosion behavior through various methods, including weight loss measurements, potentiodynamic polarization (Tafel), and electrochemical impedance spectroscopy (EIS). Additionally, the surface characteristics of the samples were examined using optical microscopy.

The primary objectives of this research are to:

1. Evaluate the Corrosion Inhibition Efficiency: Determine the effectiveness of $N(CH_3)_4^+$ OH^- in reducing the corrosion rate of API 5L X70 steel in 0.5M H_2SO_4.
2. Understand the Inhibition Mechanism: Analyze how the inhibitor molecules interact with the steel surface and form protective layers.
3. Characterize Surface Morphology: Use optical microscopy to visualize changes in the steel surface before and after inhibition treatment.
4. Develop Practical Insights: Provide insights that can aid in applying TMAOH derivatives as corrosion inhibitors in industrial settings.

Through this investigation, we aim to contribute to the broader understanding of corrosion inhibition and provide a basis for the practical use of TMAOH and its derivatives in protecting steel materials in acidic environments.

2. Experimental Methods

2.1. Material and medium

The steel under investigation is API 5L X70, a high-strength low alloy pipeline steel commonly used in the oil and gas industry. Its chemical composition, determined using spark emission spectroscopy, is detailed in Table 1. The chemical composition includes a variety of alloying elements that contribute to the steel's mechanical properties and corrosion resistance.

Table 1. Chemical Composition of API 5L X70 Steel

Elements	**C**	**Si**	**Mn**	**P**	**S**	**Cr**	**Mo**	**Ni**	**Al**
w (%)	0.0844	0.374	1.665	0.0131	0.0025	0.0475	0.0068	0.031	0.0393
B	**Cu**	**Nb**	**Ti**	**V**	**W**	**N**	**Fe**	**Ce**	**Co**
0.0014	0.0193	0.0515	0.007	0.0874	0.007	0.001	97.4	0.200	0.0098

The inhibitor utilized in this research is Tetramethylammonium hydroxide (TMAOH), supplied by Sigma-Aldrich. TMAOH is known for its effectiveness in corrosion inhibition due to its chemical structure, which is illustrated in Fig. 1. The study was conducted in a 0.5 M H_2SO_4 solution, both in the absence and presence of TMAOH at concentrations of 10^{-1}, 10^{-2}, and
10^{-3} M.

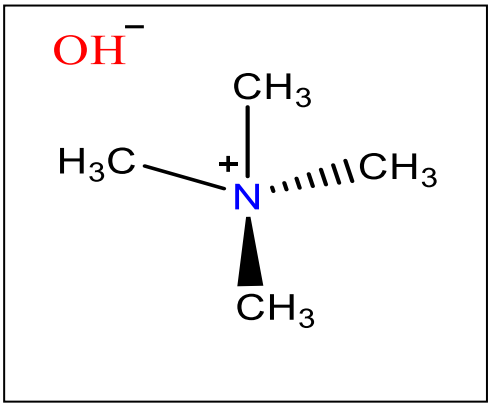

Figure 1. Chemical structure of Tetramethylammonium hydroxide.

2.2. Gravimetric Study

Gravimetric measurements were performed to assess the weight loss of steel samples due to corrosion. Samples with dimensions of 1.3 cm x 1.4 cm x 0.5 cm were immersed in 50 ml of 0.5 M H_2SO_4 solution, both with and without various concentrations of the TMAOH inhibitor. After 2 hours of immersion at 298 K, the samples were carefully removed, rinsed with distilled water and acetone to remove any residual acid or corrosion products, dried, and weighed using a KERN ALS 220-4N analytical balance with a precision of ± 0.1 mg. The weight loss data were used to calculate the corrosion rate and the inhibition efficiency of TMAOH.

2.3. Electrochemical Measurements

Electrochemical measurements were conducted to further understand the corrosion inhibition mechanism of TMAOH. These measurements were carried out using a Gamry Interface 600 potentiostat/galvanostat, controlled by Gamry Framework software. The experiments utilized a classic three-electrode electrochemical cell (Fig. 2) consisting of:

- A saturated calomel electrode (SCE) as the reference electrode.
- A platinum wire as the counter electrode.
- An API 5L X70 steel electrode as the working electrode, coated in epoxy resin to expose a flat surface area of 0.5 cm^2.

The working electrode was prepared by polishing it sequentially with silicon carbide (SiC)

abrasive papers of different grades (600, 800, 1200, 2400, and 4000), followed by polishing with a 3 µm diamond paste. The electrode was then thoroughly cleaned with distilled water, degreased with acetone, rinsed again with distilled water, and dried under a stream of dry air.
Electrochemical measurements were conducted after a half-hour of immersion at 298 K to ensure stabilization of the electrode potential. The following procedures were employed:
- Polarization Curves (Tafel): These were recorded by sweeping the potential from -250 mV to +250 mV versus SCE at a scan rate of 1 mV/s. Tafel extrapolation was used to determine the corrosion current density and the corrosion potential.
- Polarization Resistance (Rp): Rp was measured from the linear polarization curves obtained by applying a small perturbation of ±10 mV around the corrosion potential.
- Electrochemical Impedance Spectroscopy (EIS): EIS measurements were carried out over a frequency range from 100 kHz to 10 mHz, with an AC amplitude of 10 mV. The impedance data were analyzed to obtain information on the charge transfer resistance and the double-layer capacitance.

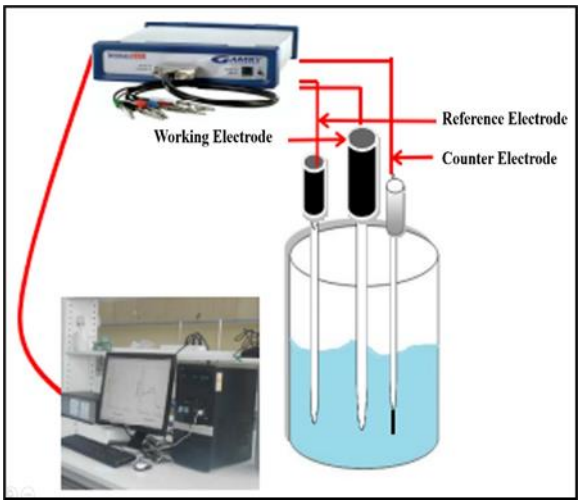

Figure 2. Classic three-electrode electrochemical cell.

2.4. Structural Characterization by Optical Microscopy

Optical microscopy was used to characterize the microstructure of API 5L X70 steel and to provide insights into the interactions at the metal/solution interface. After 72 hours of immersion in 0.5 M H_2SO_4, both without and with TMAOH, the steel samples were examined using a Nikon ECLIPSE LV 100ND optical microscope. Prior to examination, the samples were chemically etched with a 3% Nital solution for 10 seconds to reveal the microstructural features. The microstructures were documented in Figs. 7, 8, and 9 illustrating the differences in surface morphology with and without the inhibitor.

3. Results and Discussion

3.1. Electrochemical Measurements

Weight loss measurements of API 5L X70 steel in 0.5M H_2SO_4, both in the absence and presence of various concentrations of TMAOH, after 2 hours of immersion at 298 K, were evaluated by the corrosion rate C_R and the inhibition efficiency E_{WL}(%), calculated using Eqs. 1 and 2 [23]:

$$C_R = \frac{\Delta W}{At} (1)$$

Where:
- ΔW: weight loss;
- A: surface area of the sample (cm²);
- t: immersion time (h).

The corrosion rate $C_R$gives an indication of how quickly the steel is corroding in the given environment. It is determined by the weight loss per unit area of the sample per unit time.

Lower values of $C_R$indicate better resistance to corrosion.

$$E_{WL}(\%) = \frac{C_{R0} - C_R}{C_{R0}} \times 100 \qquad (2)$$

Where C_{R0} and $C_R$are the corrosion rates (mg cm^{-2} h^{-1})without and with the addition of the inhibitor in 0.5M H_2SO_4, respectively. The inhibition efficiency E_{WL}(%)measures the effectiveness of the inhibitor in reducing the corrosion rate. Higher E_{WL}(%) values indicate greater inhibition efficiency.

The calculated values of the corrosion rate (CR) and inhibition efficiency E_{WL}(%) are presented in Table 2.

Table 2. Corrosion rate (C_R) values and inhibition efficiency E_{WL}(%) obtained from gravimetric measurements

[C] M	C_R (mg. cm^{-2}. h^{-1})	E_{WL} %
Blank	0.2420	-
10^{-3}	0.0616	88.35
10^{-2}	0.0741	83.24
10^{-1}	0.0945	65.30

The results from Table 2 show that decreasing the concentration of the inhibitor reduces the corrosion rate, consequently increasing the inhibitory efficiency, which reaches a maximum value of 88.35% at 10^{-3} M. This increase is attributed to the adsorption of TMAOH molecules on the steel surface, leading to the formation of a protective film [23].

3.2. Open Circuit Potential (OCP) Monitoring of API 5L X70 Steel in 0.5M H2SO4 in the Absence and Presence of TMAOH

Before studying the electrochemical behavior of the steel, it is important to evaluate its open circuit potential (OCP) over time in 0.5M H_2SO_4 in the absence and presence of TMAOH at 20°C. The OCP was monitored at concentrations of 10^{-3}, 10^{-2}, and 10^{-1} M for 30 minutes. The evolution of the OCP characterizes the corrosion behavior of the sample and helps to achieve a relatively stable potential. This stable potential is essential for further electrochemical measurements, such as potentiodynamic polarization curves and electrochemical impedance spectroscopy.

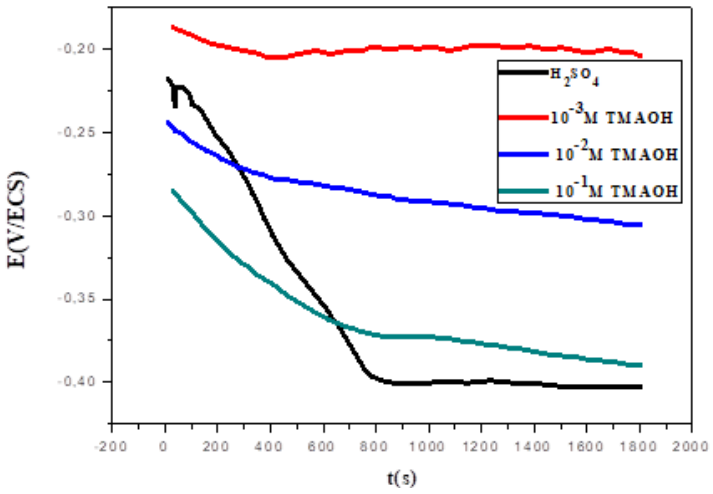

Figure 3. Open circuit potential monitoring of X70 steel immersed in 0.5M H_2SO_4 in the absence and presence of TMAOH at different concentrations.

The OCP measurements (Fig. 3) show that in the absence of the inhibitor, the OCP stabilizes after approximately 1500 seconds at a value of -0.40 V/Ag/AgCl. The addition of TMAOH

shifts the OCP towards more positive values. This shift towards more noble potentials in the presence of the inhibitor indicates the formation of a protective film on the steel surface.

3.3. Electrochemical Impedance Spectroscopy Measurements

Electrochemical impedance spectroscopy (EIS) was used to further study the corrosion behavior of API 5L X70 steel in 0.5M H_2SO_4. The Nyquist plots were obtained after 1800 seconds of immersion, both in the absence and presence of TMAOH at concentrations of 10^{-1}, 10^{-2}, and 10^{-3} M.

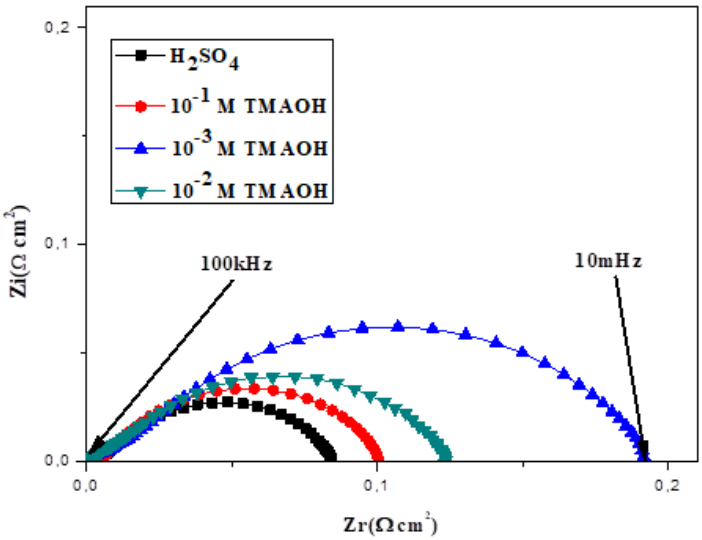

Figure 4. Nyquist plots of X70 steel in 0.5M H_2SO_4 containing different concentrations of TMAOH.

The Nyquist plots (Figure 4) reveal a single capacitive semicircular loop for both the blank solution and the TMAOH-containing solutions. This semicircular loop is characteristic of the charge transfer reaction that occurs at the steel/solution interface [24]. The diameter of the semicircle increases with the decrease of TMAOH concentration, indicating an increase in charge transfer resistance (Rp) and hence a decrease in the corrosion rate.

The equivalent electrical circuit used to simulate the metal/solution interface is shown in Figure 5. The circuit consists of the solution resistance (Rs), a constant phase element (CPE), and the charge transfer resistance (Rp). The constant phase element (CPE) is used to account for the non-ideal capacitive behavior of the double layer at the interface.

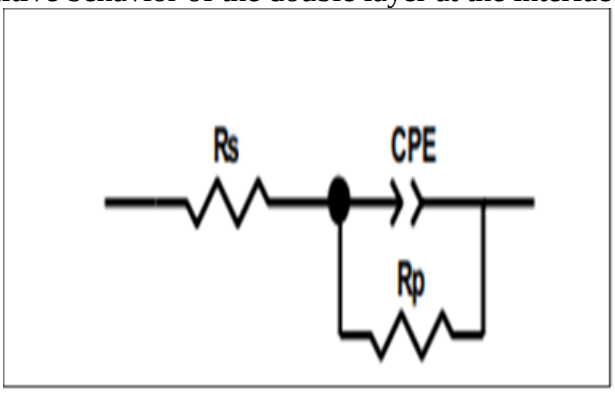

Figure 5. Equivalent electrical circuit scheme to simulate the MS/solution interface.

The addition of TMAOH, indicating the presence of a protective layer on the MS substrate. This behavior reveals that the charge transfer process is reduced due to the adsorption of TMAOH on the MS surface. It reveals a better corrosion resistance property of MS, and also provides confirmation that the charge exchange between the MS and 0.5 M H_2SO_4 is substantially reduced using TMAOH. In a similar sense, the impedance diagram without of TMAOH is the same in the case of presence of TMAOH. This allows us to observe that the

corrosion process has not been affected by the TMAOH [25,26]. As seen in Fig. 5, the electrical circuit components are Rs, CPE, and Rp. The ZCPE is calculated by Eq. 3 [27,28]:

$$Z_{CPE} = \frac{1}{Y_0(jw)^n} \quad (3)$$

With j, w, and n are imaginary unit Y_0 ($j^2 = -1$), phase shift parameter ($n=2\alpha/(\pi)$), angular frequency, and quantity of CPE, respectively. The Cdl is given by Eq. (4).

$$C_{dl} = (Y_0 R_P^{n-1})^{1/2} \quad (4)$$

Table 2 presents the values of various electrochemical parameters derived from the fitting of the impedance spectra. The corrosion inhibition efficiencies are calculated from the *Rct* values using Eq. 5 [29]:

$$\%E = \frac{(R_{ct} - R_{ct0})}{R_{ct}} \times 100 \quad (5)$$

Where R_{ct0} and R_ct represent the charge transfer resistance values of steel without and with the inhibitor, respectively.

The analysis of these parameters reveals several key findings:

- The value of R_ct increases as the inhibitor concentration decreases, suggesting the formation of a protective film at the metal/solution interface, which enhances inhibitory efficiency [30].
- The decrease in CPE values may be attributed to the increase in the thickness of the inhibitor film on the metal surface. This could result from the adsorption of TMAOH molecules at the metal/solution interface or a reduction in the local dielectric constant [31].

The maximum R_ct (953.1 Ω.cm²) and the minimum CPE (102.5 µF·cm⁻²) are achieved at a TMAOH concentration of 10^{-3} M. The inhibitory efficiency, calculated using Eq. 5, increases with decreasing TMAOH concentration, reaching a maximum value of 85.88% at 10^{-3} M.

Table 2. Calculated inhibitory efficiencies and electrochemical parameters derived from the electrical circuit of X70 steel in 0.5M H_2SO_4 in the absence and presence of TMAOH.

Inhibitor Concentration (M)	**R_s ($\Omega.cm^2$)**	**R_{ct} ($\Omega.cm^2$)**	**CPE ($\mu F.cm^{-2}$)**	**n**	**E (%)**
H_2SO_4 à 0.5 M	2.17	94.39	749.4	0.88	-
10^{-1}	3.31	303.6	202.7	0.89	68.90
10^{-2}	3.42	424.8	179.4	0.87	77.78
10^{-3}	3.83	953.1	102. 5	0.90	85.88

3.4.Potentiodynamic (Tafel) Polarization

Fig. 6 shows the Tafel polarization curves of the samples in 0.5M H_2SO_4, both in the absence and presence of TMAOH at different concentrations after 1800 seconds of immersion at 298K. The curves exhibit a similar general shape, with an anodic passivation stage n the potential range between -0.2 and -0.1 V/SCE.

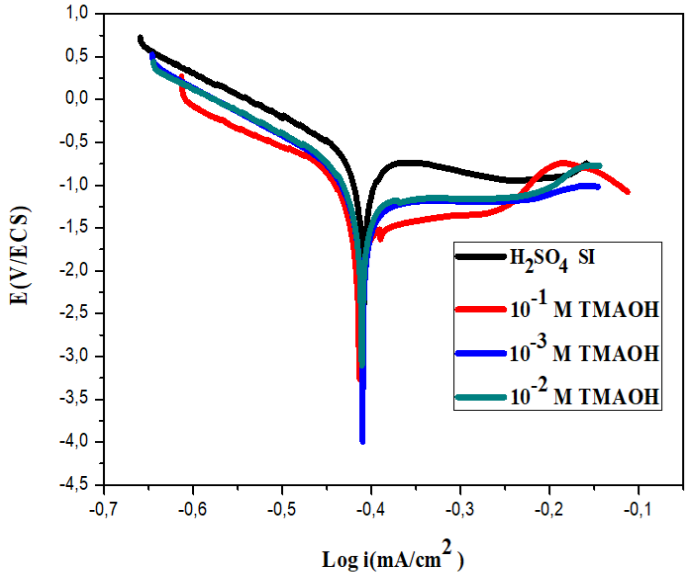

Figure 6. Tafel polarization curves of X70 steel in 0.5M H_2SO_4 containing different concentrations of TMAOH

The addition of the inhibitor results in a reduction of both anodic and cathodic current densities, a shift of the corrosion potential towards more noble values, and variations in the βc and βa values. This affects the kinetics of the cathodic reaction and the adsorption of inhibitor molecules on the metal surface.

The classification of an inhibitor typically depends on its influence on the displacement of the corrosion potential (d_{Ecorr}) relative to its value without the inhibitor (Ecorr). If d_{Ecorr}> 85 mV, the inhibitor is considered either anodic or cathodic. If d_{Ecorr}< 85 mV, it is considered a mixed-type inhibitor [32, 33].

In this study, d_{Ecorr} = +53 mV towards the anodic direction, indicating that TMAOH acts as a mixed inhibitor with a predominantly anodic effect. This behavior is due to the adsorption of TMAOH molecules, which block both cathodic and anodic active sites by reducing the rate of cathodic hydrogen evolution and slowing down the anodic metal dissolution reactions [34].

Table 3 summarizes the electrochemical parameters derived from the Tafel polarization curves, including corrosion potential (E_{corr}), cathodic Tafel slope (βc), anodic Tafel slope (βa), corrosion current density (i_{corr}), and polarization resistance (Rp) measured using the linear polarization resistance (LPR) method. Without the inhibitor, icorr = 64.59 µA·cm^{-2} and Rp = 104.28 Ω·cm², which reach 4.41 µA·cm^{-2} and 867.4 Ω·cm² at 10^{-3} M TMAOH, respectively.

Table 3. Calculated inhibition efficiencies and electrochemical parameters derived from the polarization curves of X70 steel in 0.5 M H_2SO_4 in the absence and presence of TMAOH.

Inhibitor Concentration (M)	**E_{corr} (mV)**	**I_{corr} (µA cm^{-2})**	**-βc (mV dec^{-1})**	**Ba (mV dec^{-1})**	**Rp(Ω cm^2)**	**E_I %**
W. I.	-401,7	64.59	114.7	66.4	104,28	-
10^{-1}	-405.4	15.83	96.0	37	325.3	77,91
10^{-2}	-306.9	11.89	86.7	52	453.02	83,02
10^{-3}	-310.6	4.41	120.8	79.4	867.4	87,28

Overall, the results from the weight loss measurements, OCP monitoring, EIS studies, and

Potentiodynamic Polarization consistently show that TMAOH is an effective corrosion inhibitor for API 5L X70 steel in 0.5M H_2SO_4. The adsorption of TMAOH on the steel surface forms a protective film that significantly reduces the corrosion rate

4. Metallographic Study

The microstructural observation using an optical microscope on the polished and chemically etched X70 steel sample revealed significant details about its composition. The analysis showed the presence of ferrite (light phase) and a relatively small amount of pearlite (dark phase), as depicted in Fig. 7. Ferrite, being a soft and ductile phase of steel, provides good mechanical properties, while pearlite, which consists of alternating layers of ferrite and cementite, offers enhanced strength and hardness.

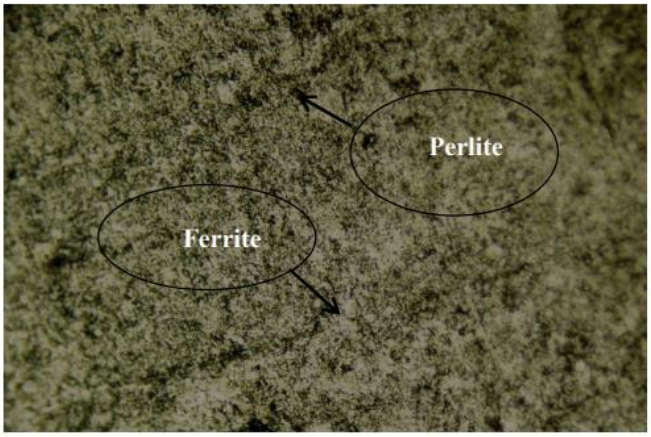

Figure 7. Metallographic observation of X70 steel

Further examination of the X70 steel sample immersed in an H_2SO_4 acidic medium revealed pronounced degradation features. The optical microscope images highlighted the formation of large pits on the surface of the X70 sample, indicative of severe corrosion. These pits are caused by the aggressive attack of sulfuric acid on the steel surface, leading to localized material loss, as illustrated in Figure 8.

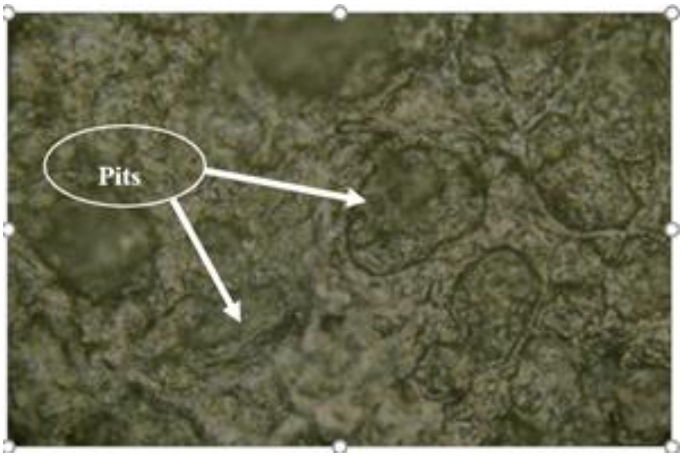

Figure 8. Metallographic observation of pits on the surface of X70 steel immersed in 0.5M H_2SO_4

To evaluate the effectiveness of corrosion inhibitors, the X70 steel sample was also immersed in an acidic solution containing an inhibitor (H_2SO_4 + TMAOH 10^{-3} M). The microstructural observations revealed significantly smaller pits on the surface compared to the sample immersed in the acidic medium without inhibitor (Fig. 8). This reduction in pit size demonstrates the role of TMAOH as an effective corrosion inhibitor, which slows down the rate of corrosion by forming a protective film on the steel surface, as shown in Fig. 9.

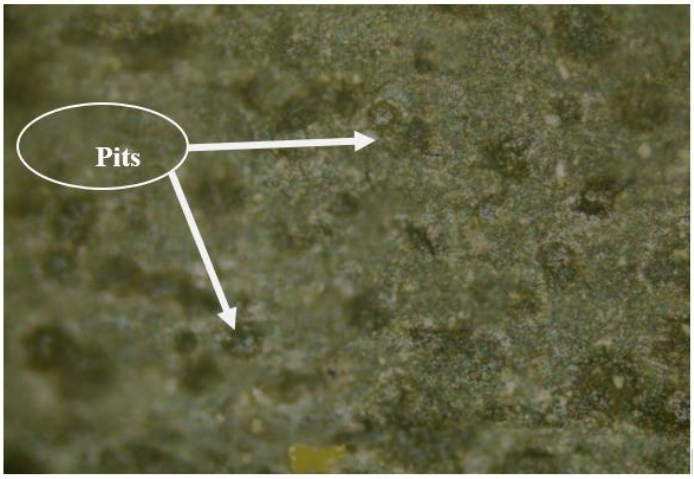

Figure 9. Metallographic observation of pits on the surface of X70 steel immersed in 0.5M H_2SO_4 + 10^{-3}M TMAOH

5. Molecular Dynamics Simulation

Molecular dynamics simulations were performed to gain insights into the interaction mechanisms between the inhibitor molecules and the Fe surface. The simulations of the two-pyrazoline derivatives were conducted in a simulation box (24.82 × 24.82 × 35.63 Å) with periodic boundary conditions using the Discover module in Materials Studio 7.0 (from Accelrys Inc.). The simulation conditions were set at 298 K with an NVT ensemble, a time step of 1 fs, and a total simulation time of 50 ps, utilizing the COMPASS force field [37].

The interaction energy $E_{interaction}$between the Fe surface and the inhibitor molecule, and the binding energy, were computed using the Eqs. 6 and 7:

$$E_{interaction} = E_{total} - \left(E_{surface+H_2O} + E_{inhibitor}\right) \quad (6)$$

$$E_{binding} = -E_{interaction} \quad (7)$$

Where the E_{total} is defined as the total energy of the entire system, $E_{surface+H_2O}$ is defined as the total energy of Fe surface and water molecule and the $E_{inhibitor}$is the energy of the adsorbed inhibitor molecule on the surface.

Figure 9. illustrates the energy and temperature equilibrium curves obtained from the MD simulation for the TMAOH molecule. The curves indicate that both energy and temperature reached a stable equilibrium, suggesting that the entire system has achieved a state of balance [38].

The equilibrium adsorption configuration of the studied inhibitor on the Fe (110) surface is depicted in Figure 9, and the calculated interaction and binding energies are listed in Table 4. The close proximity of the inhibitor molecules to the Fe surface, as observed in Figure 9, suggests strong adsorption. The highly negative binding energy values indicate that the adsorption process is spontaneous, strong, and stable [39].

Table 4: Interaction energies between the inhibitor and Fe (110) surface in an aqueous phase (kJ/mol)

System	Binding energy	ıteraction energy
Fe (110)+TMAOH	924,285	-924,285

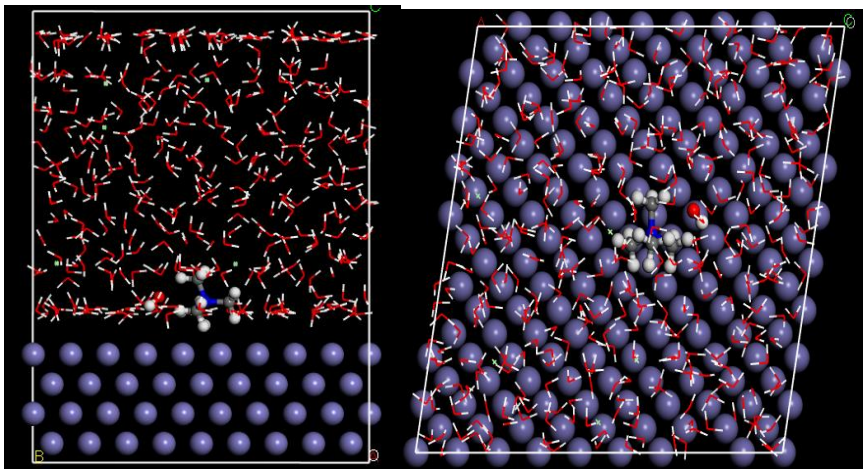

Figure 9. Equilibrium adsorption configurations of TMAOH on Fe (110) surface in water solution (top and side view)

Conclusion

The inhibition of X70 steel corrosion by TMAOH in 0.5M H_2SO_4 was studied using various analytical techniques including gravimetric measurements, potentiodynamic polarization (Tafel) methods, electrochemical impedance spectroscopy (EIS), and optical microscopy observations. The comprehensive results obtained from these methods lead to several important conclusions:

- TMAOH exhibits excellent inhibitory properties, with an efficiency of 87.28% at a concentration of 10^{-3} M. This high efficiency highlights its potential as a viable corrosion inhibitor for steel in acidic environments.
- TMAOH acts as a mixed-type inhibitor, primarily exhibiting anodic inhibition. This means that TMAOH not only reduces the anodic reaction rate but also has some effect on the cathodic reaction, thereby providing a comprehensive protective effect.
- A decrease in the concentration of the inhibitor results in an increase in charge transfer resistance.
- The optical microscopy observations confirm the formation of an inhibitor film on the steel surface. This film acts as a physical barrier, preventing direct contact between the steel and the corrosive environment, thereby reducing the rate of corrosion.
- Molecular dynamics simulations provide valuable insights into the interaction between

the TMAOH inhibitor and the Fe surface. The high negative binding energy values obtained from these simulations indicate that the adsorption of TMAOH on the Fe (110) surface is spontaneous, strong, and stable. This supports the experimental findings and demonstrates the effectiveness of TMAOH at a molecular level in preventing corrosion.

These findings underscore the effectiveness of TMAOH as a corrosion inhibitor for X70 steel in sulfuric acid media, providing valuable insights for its practical application in industry.

References

[1] Shishir Pandya, K.S.Ramakrishna, A.Raja Annamalai and Anish Upadhyaya, Effect of sintering temperature on the mechanical and electrochemical properties of austenitic stainless steel, *Mater. Sci. Eng., A, 556*(2012), p. 271.

[2] Guanshun BAI,Shanping Lu, Dianzhong Li andYiyi Li, Influences of niobium and solution treatment temperature on pitting corrosion behaviour of stabilised austenitic stainless steels. *Corros. Sci.*, 108(2016), p. 111.

[3] Magdy A.M. Ibrahim, SS Abd El Rehim and M. M. Hamza, Corrosion behavior of some austenitic stainless steels in chloride environments, *Mater. Chem. Phys.*, 115(2009), No.1,p.80.

[4] M. Mehdipour, R. Naderi and B. P. Markhali, Electrochemical study of effect of the concentration of azole derivatives on corrosion behavior of stainless steel in H_2SO_4, *Prog. Org. Coat.*, 77 (2014),No.11, p 1761.

[5] M.Yadav, S. Kumar , T. Purkait, , L. O. Olasunkanmi, I. Bahadur and E. E. Ebenso,. Electrochemical, thermodynamic and quantum chemical studies of synthesized benzimidazole derivatives as corrosion inhibitors for N80 steel in hydrochloric acid, *J. Mol. Liq.*, 213(2016), p.122.

[6] Chandrabhan Verma, E.E. Ebenso, I. Bahadur , I.B. Obot and M.A. Quraishi, 5-(Phenylthio)-3H-pyrrole-4-carbonitriles as effective corrosion inhibitors for mild steel in 1M HCl, Experimental and theoretical investigation, *J. Mol. Liq.,212*(2015), p. 209.

[7] HulyaKeles and Mustafa Keles, Electrochemical investigation of a schiff base synthesized by cinnamaldehyde as corrosion inhibitor on mild steel in acidic medium, *Res. Chem. Intermed*., 40(2014), No.1, p.193.

[8] G. Karthik, M. Sundaravadivelu and P. Rajkumar, Corrosion inhibition and adsorption properties of pharmaceutically active compound esomeprazole on mild steel in hydrochloric acid solution, *Res. Chem. Intermed*., 41(2015), No.3, p.1543.

[9] Mohamed Gobara, Ahmad Baraka and BasemZaghloul, Inhibition of mild steel corrosion in sulfuric acid solution using collagen, *Res. Chem. Intermed*., No.10, 41(2015), p. 7245.

[10] A. Kosari, M.H. Moayed, A. Davoodi, R. Parvizi, M. Momeni, H. Eshghi and H. Moradi, Electrochemical and quantum chemical assessment of two organic compounds from pyridine derivatives as corrosion inhibitors for mild steel in HCl solution under stagnant condition and hydrodynamic flow, *Corros. Sci*., 78(2014), p.138.

[11] Sam John, R. Jeevana, K.K. Aravindakshan and Abraham Joseph, Corrosion inhibition of mild steel by N (4)-substituted thiosemicarbazone in hydrochloric acid media, *Egypt. J. Pet.*, (2016)

[12] MahendraYadav, LaldeepGope and TarunKanti Sarkar, Synthesized amino acid compounds as eco-friendly corrosion inhibitors for mild steel in hydrochloric acid solution, electrochemical and quantum studies, *Res. Chem. Intermed*., No.3, 42(2016), p.2641.

[13] K.R. Ansari, M.A. Quraishi and, Ambrish Singh, Pyridine derivatives as corrosion inhibitors for N80 steel in 15% HCl: Electrochemical, surface and quantum chemical studies, *Meas*., 76 (2015), p.136.

[14] Ayşe OngunYüce, EsraTelli, BaşakDoğruMert, GülfezaKardaş and BirgülYazıcı, Experimental and quantum chemical studies on corrosion inhibition effect of 5, 5 diphenyl 2-thiohydantoin on mild steel in HCl solution, *J. Mol. Liq*., 218(2016), p.384.
[15] R. Yıldız, A. Döner, T. Doğan and İ. Dehri. Experimental studies of 2-pyridinecarbonitrile as corrosion inhibitor for mild steel in hydrochloric acid solution, *Corros. Sci*., 82(2014), p.125.
[16] Bin Xu, Yan Ji, Xueqiong Zhang, XiaodongJin,Wenzhong Yang and Yizhong Chen, Experimental and theoretical evaluation of N, N-Bis (2-pyridylmethyl) aniline as a novel corrosion inhibitor for mild steel in hydrochloric acid, *J. Taiwan Inst. Chem. Eng*., 59(2016), p. 526.
[17]KoraySayin, Hojat Jafari and Farhadmohsenifar ,Effect of pyridyl on adsorption behavior and corrosion inhibition of aminotriazole, *J. Taiwan Inst. Chem. Eng*., 68 (2016), p. 431-439.
[18] S. Belkaid, K. Tebbji, A.Mansri, A. Chetouani and BelkheirHammouti, Poly (4-vinylpyridine-hexadecyl bromide) as corrosion inhibitor for mild steel in acid chloride solution, *Res. Chem. Intermed.*, 38(2012), No.9, p. 2309.
[19] A. Ghazoui, R. Saddik, B. Hammouti, A. Zarrouk, N. Benchat, M. Guenbour, S. S. Al-Deyaband I.Warad, Inhibitive effect of imidazopyridine derivative towards corrosion of C38 steel in hydrochloric acid solution, *Res. Chem. Intermed*., 39 (2013), No.6, p. 2369-2377.
[20] *R. Karthik, G. Vimaladevi, Shen-Ming Chen, A. Elangovan, B. Jeyaprabha and P. Prakash,* Corrosion Inhibition and Adsorption Behavior of 4–Amino Acetophenone Pyridine 2-Aldehyde in 1 M Hydrochloric Acid, *Int. J. Electrochem. Sci*., 10 (2015), p. 4666.
[21] K. R.Ansari, M. A. Quraishi and Ambrish Singh, Corrosion inhibition of mild steel in hydrochloric acid by some pyridine derivatives, An experimental and quantum chemical study, *J. Ind. Eng. Chem*., 25 (2015), p. 89.
[22]K. Abderrahim , T. Chouchane , I. Selatnia, , A. Sid, P. Mosset; Evaluation of the effect of Tetramethylammonium hydroxide on the corrosion inhibition of A9M steel in industrial water: an experimental, morphological and MD simulation insights.Chemical Data Collections 28 (2020) 100391
[23] K. Abderrahim , I. Selatnia , A. Sid , P. Mosset ;1,2-bis(4-chlorobenzylidene)Azine as new and effective corrosion inhibitor for copper in 0.1 N HCl: A combined experimental and theoretical approach ,Chemical Physics Letters 707 (2018) 117–128
[24] F. Benhiba,R. Hsissou and K. Abderrahim; Development of New Pyrimidine Derivative Inhibitor for Mild Steel Corrosion in Acid Medium. Journal of Bio- and Tribo-Corrosion (2022) 8:36 https://doi.org/10.1007/s40735-022-00637-5
[25] Wang D, Li Y, Chen B, Zhang L (2020) Novel surfactants as green corrosion inhibitors for mild steel in 15% HCl: experimental and theoretical studies. Chem Eng J 402:126219
[26] Ma Q, Qi S, He X, Tang Y, Lu G (2017) 1,2,3-Triazole derivatives as corrosion inhibitors for mild steel in acidic medium: experimental and computational chemistry studies. Corros Sci 129:91–101
[27] Solomon MM, Gerengi H, Kaya T, Umoren SA (2017) Performance evaluation of a chitosan/silver nanoparticles composite on St37 steel corrosion in a 15% HCl solution. ACS Sustain Chem Eng 5:809–820
[28] Ansari KR, Chauhan DS, Quraishi MA, Saleh TA (2020) Bis (2-Aminoethyl) amine-modifed graphene oxide nanoemulsion for carbon steel protection in 15% HCl: efect of temperature and synergism with iodide ions. J Colloid Interface Sci 564:124–133
[29] C.Verma, M.A.Quraishi and A.Singh, 2-Amino-5-nitro-4, 6-diarylcyclohex-1-ene-1, 3, 3-tricarbonitriles as new and effective corrosion inhibitors for mild steel in 1M HCl: Experimental and theoretical studies, *J. Mol. Liq.,212*(2015), p.804.

[30]P. B.Raja, A.A. Rahim, H. Osman and K. Awang, Inhibitive effect of Xylopiaferruginea extract on the corrosion of mild steel in 1M HCl medium, *Int. J. Miner. Metall. Mater*., 18(2011), No.4, p. 413.
[31]I. B.Obot and A.Madhankumar, Synergistic effect of iodide ion addition on the inhibition of mild steel corrosion in 1 M HCl by 3-amino-2-methylbenzylalcohol, *Mater. Chem. Phys*., 177(2016), p. 266.
[32] M. El Faydy, M. Galai, A. El Assyry, A. Tazouti, R. Touir, B. Lakhrissi, M. EbnTouhami, and A. Zarrouk, Experimental investigation on the corrosion inhibition of carbon steel by 5-(chloromethyl)-8-quinolinol hydrochloride in hydrochloric acid solution, *J. Mol. Liq.,* 219(2016), p.396.
[33] M. Pitchaipillai, K. Raj, J.Balasubramanian and P.Periakaruppan, Benevolent behavior of Kleinia grandiflora leaf extract as a green corrosion inhibitor for mild steel in sulfuric acid solution, *Int. J. Miner. Metall. Mater*., 21(2014), No.11, p.1083.
[34] HulyaKeles and Mustafa Keles, Electrochemical investigation of a schiff base synthesized by cinnamaldehyde as corrosion inhibitor on mild steel in acidic medium, *Res. Chem. Intermed*., 40(2014), No.1, p.193.
[35] V. Srivastava, J. Haque, C. Verma, P. Singh, H. Lgaz, R. Salghi, M. Quraishi, Amino acid based imidazolium zwitterions as novel and green corrosion inhibitors for mild steel: Experimental, DFT and MD studies, Journal of Molecular Liquids, 244 (2017) 340-352.
[36]H. Lgaz, R. Salghi, K.S. Bhat, A. Chaouiki, S. Jodeh, Correlated experimental and theoretical study on inhibition behavior of novel quinoline derivatives for the corrosion of mild steel in hydrochloric acid solution, Journal of Molecular Liquids, 244 (2017) 154-168.

[37]H. Sun, COMPASS: an ab initio force-field optimized for condensed-phase applications overview with details on alkane and benzene compounds, The Journal of Physical Chemistry B, 102 (1998) 7338-7364.
[38]Z. Zhang, N. Tian, X. Huang, W. Shang, L. Wu, Synergistic inhibition of carbon steel corrosion in 0.5 M HCl solution by indigo carmine and some cationic organic compounds: experimental and theoretical studies, RSC Advances, 6 (2016) 22250-22268.
[39] J. Zeng, J. Zhang, X. Gong, Molecular dynamics simulation of interaction between benzotriazoles and cuprous oxide crystal, Computational and Theoretical Chemistry, 963 (2011) 110-114.